

ORIGINAL ARTICLE

AMPK α 2 knockout enhances tumour inflammation through exacerbated liver injury and energy deprivation-associated AMPK α 1 activation

Shulan Qiu¹ | Taoyan Liu¹ | Chunmei Piao¹ | Ying Wang¹ | Kefang Wang¹ |
Yandong Zhou² | Lun Cai¹ | Shuai Zheng¹ | Feng Lan¹  | Jie Du¹

¹Beijing Institute of Heart, Lung and Blood Vessel Diseases, AnZhen Hospital, Capital Medical University, Beijing, China

²Department of Cellular and Molecular Physiology, Penn State University College of Medicine, Hershey, Pennsylvania

Correspondence

Feng Lan, PhD and Jie Du, PhD, Beijing Anzhen Hospital, Beijing, China.
Email: fenglan@ccmu.edu.cn;
jiedubj@126.com

Present addresses

Shulan Qiu, Department of Molecular Medicine, Barshop Institute for Longevity and Aging Studies, University of Texas Health Science Center, San Antonio, Texas.

Ying Wang, Department of Biochemistry and Molecular Biology, Mayo Clinic, Jacksonville, Florida.

Funding information

Wu Jieping Medical Foundation, Grant/Award Number: 320675017016; National Natural Science Foundation of China, Grant/Award Number: 81400194, 81570215, 81570662, 81770468

Abstract

Tissue damage and its associated-inflammation act as tumour initiators or propagators. AMP-activated protein kinase (AMPK) is activated by environmental or nutritional stress factors, such as hypoxia, glucose deprivation, and other cell injury factors, to regulate cell energy balance and differentiation. We previously have reported that AMPK α 2 deficiency resulted in the energy deprivation in tumour-bearing liver and the enhanced-hepatocyte death. In this study, AMPK α 2 knockout mice and the liver metastasis model of colon cancer cells were used to address the role of AMPK α isoforms in tumour inflammation. First, we found that the AMPK α 2 deficiency exacerbated the liver injury and recruitment of macrophages. Meanwhile, although compensatory expression of AMPK α 1 was not significant after AMPK α 2 knockout, AMPK α 1 phosphorylation was elevated in remnant liver in AMPK α 2 knockout mice, which was positively associated with the enhanced energy deprivation in the AMPK α 2 deficient mice. Furthermore, the activated AMPK α 1 in macrophage contributed to its polarizing to tumour-associated phenotype. Thus, the enhanced tumour-associated inflammation and activation of AMPK α 1 in the AMPK α 2 deficient mice may exacerbate the tumour development by affecting the tumour inflammatory microenvironment. Our study suggests that the two isoforms of AMPK α , AMPK α 1 and AMPK α 2 play different roles in controlling tumour development.

KEYWORDS

AMPK α 1, AMPK α 2 deficiency, energy deprivation, liver metastasis, macrophages

1 | INTRODUCTION

AMP-activated protein kinase (AMPK) is a sensor and regulator activated by several factors, such as energy, nutritional, oxidative

injury.¹⁻⁶ The two isoforms (α 1 and α 2) of AMPK catalytic subunit are enriched in specific tissues and cells. AMPK α 1 is enriched in spleen and brain, but AMPK α 2 is enriched in liver, skeletal muscle, kidney, and heart.⁷⁻⁹ Furthermore, AMPK α 1 is localized predominantly in the cytoplasm, while AMPK α 2 is localized in both the nucleus and the cytoplasm.¹⁰⁻¹³ Previous studies also suggest that AMPK α 1 and α 2 catalytic subunits have different physiological

Shulan Qiu and Taoyan Liu contributed equally to this work.

This is an open access article under the terms of the Creative Commons Attribution License, which permits use, distribution and reproduction in any medium, provided the original work is properly cited.

© 2018 The Authors. Journal of Cellular and Molecular Medicine published by John Wiley & Sons Ltd and Foundation for Cellular and Molecular Medicine.

roles, for example, AMPK α 2 but not AMPK α 1 affects the whole-body energy metabolism and insulin sensitivity. However, there are limited studies focusing on whether AMPK α 1 or AMPK α 2 in different cells have similar or different functions during tumour development.

The stresses from a tumour, including energy/nutrient competition and inflammation, can result in the death of healthy cells. The insufficient clearance of dead cells by phagocytes can lead to pathological inflammation,¹⁴ which further promote the development of tumour.^{15,16} Our previous study showed that hepatocyte enriches AMPK α 2 and liver metastasis results in glucose deprivation and necrosis of liver hepatocytes.¹⁷ AMPK α 2 deficiency significantly aggravated the glucose deprivation and necrosis of hepatocytes via increased ROS production. However, the role of AMPK in liver injury and inflammation remains unclear.

Although both tumour-promoting and tumour-antagonizing immune cells are present in the tumour microenvironment, cancer cells prefer to invoke the immune system facilitating the recruitment, activation, and persistence of the tumour-promoting immune cells.^{18,19} The polarization of macrophages is one of the prominent events after leucocyte infiltration into the tumour microenvironment. Macrophages differentiate into tumour-associated macrophages (TAMs), ie, "M2-like" phenotypes, in response to distinct signals such as interleukin-4 (IL-4), IL-10, IL-13 from Th2 cells, regulatory T cells (Tregs) in tumour tissues.^{20,21} Abundant shreds of evidence demonstrate that TAMs are associated with poor prognosis for various types of cancer in both clinics as well as experimental animal tumour models.²²⁻²⁴ TAMs are known to facilitate the tumour metastasis, tumour-associated angiogenesis and tumour cell invasion.^{16,25} AMPK in macrophages can be activated with anti-inflammatory cytokines, whereas pro-inflammatory stimulus results in the inactivation of AMPK, and AMPK is suggested to promote macrophage polarization to an M2 functional phenotype.²⁶⁻²⁸ Metabolic shifts, including lower glycolytic rates, increased glucose uptake and glycolysis, have been reported in anti-inflammatory cells, such as M2 macrophages, Tregs, and quiescent memory T cells.^{29,30} Altered metabolism may thus participate in the differentiation of inflammation programmes. We previously reported that AMPK α 2 deficiency increased glucose deprivation in tumour-bearing liver¹⁷ and glucose deprivation also existed in the large tumour masses.³¹ However, it remains unclear whether and how the energy stress in tumour microenvironment contributes to macrophage polarization.

Liver tissue is susceptible for tumour origination or metastasis and is abundant with AMPK α 2. Our previous study has shown that the metastasis of colon cancer cells in liver resulted in hepatocyte necrosis through energy deprivation but not only because of the space conflict.¹⁷ In this study, we further exploited the role of AMPK α 1/ α 2 isoforms in energy deprivation, liver injury, and macrophage polarization. Our results showed that AMPK α 2 and AMPK α 1 in distinct types of cells in the tumour microenvironment play different roles.

2 | MATERIALS AND METHODS

2.1 | Mouse tumour models

A liver metastasis model was carried out as described previously.¹⁷ SL4-luciferase cells, a mouse colon carcinoma cell line with constitutive luciferase expression, were used for this model. SL4 cell line was transfected with a vector expressing luciferase and G418 was used for screening the stably transfected cell strain. Then the intraperitoneal injection of D-Luciferin can show the tumour location and size. Briefly, 5×10^5 SL4 cells in 100 μ L of DMEM/F12 medium were intrasplenically injected into the spleen with a 26-gauge needle after the mice were anaesthetized by intraperitoneal injection with pentobarbital (100 mg/kg). Mice were killed at the indicated day, and the blood, spleen, and liver with tumour were harvested after heart perfusion with saline. All the mice were housed in standard cages with a constant temperature range of $22 \pm 2^\circ\text{C}$, 60% relative humidity and an artificial 12-hour light/dark cycle. The study conforms to the Guide for the Care and Use of Laboratory Animals published by the U.S. National Institutes of Health (NIH publication No. 8523, revised 1996), and the protocol were approved by the Institutional Animal Care and Use Committee at Capital Medical University.

2.2 | Tumour analysis

D-Luciferin (15 mg/mL) was intraperitoneally injected at a dose of 10 μ L/g of mouse bodyweight just before analysis. The tumour size was analysed by a Xenogen-IVIS Lumina II device (Caliper Life Sciences, Hopkinton, MA, USA) 30 minutes after injection of 2-Deoxyglucosone 750.

2.3 | Alanine aminotransferase (ALT)/aspartate aminotransferase (AST) activity measurement

Fasting blood was collected from the heart of mice and then centrifuged at the speed of 1000 g for 5 minutes at room temperature. The activities of AST and ALT were measured by Automatic Analyzer 7020 (Hitachi, Tokyo, Japan) with the ALT, AST assay kit (BioSino Biotechnology & Science Inc., Beijing, China).

2.4 | Flow cytometry

The composition of inflammatory cells was quantified by flow cytometry as described.³² Briefly, tumour tissues were cut into multiple small cubes and digested in an enzyme mixture containing collagenase type I (0.05 mg/mL) and type IV (0.05 mg/mL) and hyaluronidase (0.025 mg/mL) and DNase I (0.01 mg/mL), and soybean trypsin inhibitor (0.01 mg/mL) in DMEM for 45 minutes at 37°C . The cell suspension was centrifuged and preincubated with fragment crystallizable- γ block antibody (anti-mouse CD16/32; PharMingen, San Diego, CA, USA) to prevent non-specific binding. Cell staining involved different combinations of fluorochrome-coupled antibodies to CD45.2, F4/80,

NK1.1, CD206, CD3, CD4, or CD8 (Invitrogen, Carlsbad, CA, USA) for 30 minutes at 4°C in the dark. Fluorescence data were collected using an EPICS XL Flow Cytometer (Beckman Coulter, Brea, CA, USA) and analysed by using of CellQuest (Beckman). Fluorescence minus one (FMO) controls were included to determine the level of non-specific staining and auto-fluorescence associated with the subset of cells in each fluorescence channel.

2.5 | Histology and immunohistochemistry

Livers from control mice and SL4-injected mice were harvested and then paraffin-sectioned and stained with haematoxylin and eosin for morphological observation. For immunohistochemistry staining, the livers sections were fixed with 4% paraformaldehyde in PBS, incubated with the primary antibodies against Mac-2 (1:200), Ki67 (1:200), CD31(1:200), and TGF β (1:200), and then incubated with the Dako ChemMate™ EnVision System (Dako, Glostrup, Denmark) for 30 minutes. Staining was visualized with use of diaminobenzidine and counterstaining with haematoxylin.

2.6 | Western blot analysis

Protein was extracted using a Protein Extraction Kit containing protease inhibitor and protein phosphatase Inhibitor Cocktail. Equal amounts of protein extract (40 μ g/lane) were separated using a 10% SDS-PAGE gel. The blot was further probed with the primary antibodies anti-GAPDH (1:1000), anti-AMPK α 1(1:1000), anti-AMPK α 2 (1:1000), p-AMPK α Thr172, and anti-AMPK α (1:1000) overnight at 4°C and then fluorescent secondary antibodies (Alexa Fluor 800; Rockland Immunochemical, Gilbertsville, PA, USA) for 1 h at room temperature. Protein expression was analysed with the Odyssey infrared imaging system and Odyssey software and normalized to GAPDH expression.

2.7 | Quantitative real-time PCR

Total RNA was extracted with Trizol reagent (Invitrogen) according to the manufacturer's protocol and 2 μ g was reversed-transcribed using the GoScript™ Reverse Transcription system (Promega, Madison, WI, USA). For real-time quantitative PCR, the iQ5 system (Bio-Rad, Hercules, CA, USA) with SYBR Green I (Takara, Kusatsu, Japan) was used. Amplification was performed at 95°C for 5 minutes, 95°C for 45 seconds and 57°C for 45 seconds of each step for 45 cycles. The housekeeping gene GAPDH was used as a control. The primers used are shown below: Tumour necrosis factor- α (TNF- α): Forward, tcttctcattctgctgttg; Reverse, ggtctggccatagaactga; inducible nitric oxide synthase (iNOS): Forward, gggctgtcacggagatca; Reverse, ccatgatggtcacattctgc; arginase-1 (Arg-1): Forward, aaagctggtctgctgga; Reverse, acagacctgggtctctac.

2.8 | Glucose mass spectrometry imaging

As described previously,³¹ fresh tumour-bearing liver tissue was snap-frozen and cryosectioned at 10 μ m thickness. The slices of WT and

AMPK α 2 KO were transferred onto the same conductive side of indium tin oxide (ITO) slides. Desiccate the slide in vacuum for 30–60 min. After drying, the matrix of N-(1-naphthyl) ethylenediamine dihydrochloride (NEDC) was applied by the Bruker ImagePrep device (Bruker Daltonics, Bremen, Germany). MALDI mass spectra were acquired at negative ion mode using a reflectron geometry MALDI-TOF mass spectrometer (Ultraflex extreme; Bruker Daltonics) equipped with a neodymium-doped yttrium aluminum garnet (Nd:YAG)/355-nm laser as the excitation source. Imaging data were analysed using FlexImaging v3.0 and FlexAnalysis v3.4. The intensity of glucose was shown as a false colour of the image from the mass spectrometry peak.

2.9 | Statistical analysis

The data are expressed as means \pm SD. Statistical analyses involved the use of GraphPad Prism v5.00 for Windows (GraphPad Software Inc., San Diego, CA, USA). Comparisons among more than two groups were analysed by one-way analysis of variance followed by the Student-Newman-Keuls test. $P < 0.05$ was considered statistically significant.

3 | RESULTS

3.1 | Metastasis of colon cancer cells in liver results in greater liver injury and macrophage recruitment

Cell death causes inflammation in cancer. Many previous studies showed that cancer caused liver injury.^{33,34} Our previous results also suggested that colon cancer liver metastasis resulted in liver injury.¹⁷ To confirm whether the liver damage is associated with liver metastasis or tumour alone, we compared the liver injury in mice bearing subcutaneous tumour or mice which have liver metastasis of colon cancer cells. Figure 1A showed the gross pictures of the subcutaneous tumour and tumour-bearing liver, and their weights were not significantly different although the liver metastasis contained the liver remnant (Figure 1B). We then examined the liver damage by measuring blood ALT and AST levels. The results showed that mice bearing liver metastasis of colon cancer cells had much higher levels of ALT and AST (subcutaneous tumour vs liver metastasis) in blood than mice with subcutaneous tumour xenograft (Figure 1C), suggesting that liver metastasis resulted in much more liver damage than the subcutaneous tumour. Since cancer increases inflammatory cells in blood,³⁵ the flow-cytometric analysis of blood cells indicated that liver metastasis caused more F4/80⁺ macrophage (Figure 1D, E) and NK1.1⁺ cells (Figure 1F, G) but not CD3⁺ T cells (Figure 1H, I) in blood, which was positively associated with the greater liver injury caused by liver metastasis.

3.2 | AMPK α 2 deficiency exacerbates liver metastasis and liver damage

Previously, we reported that AMPK α 2 deficiency significantly increased the liver injury and hepatocyte death.¹⁷ However, those

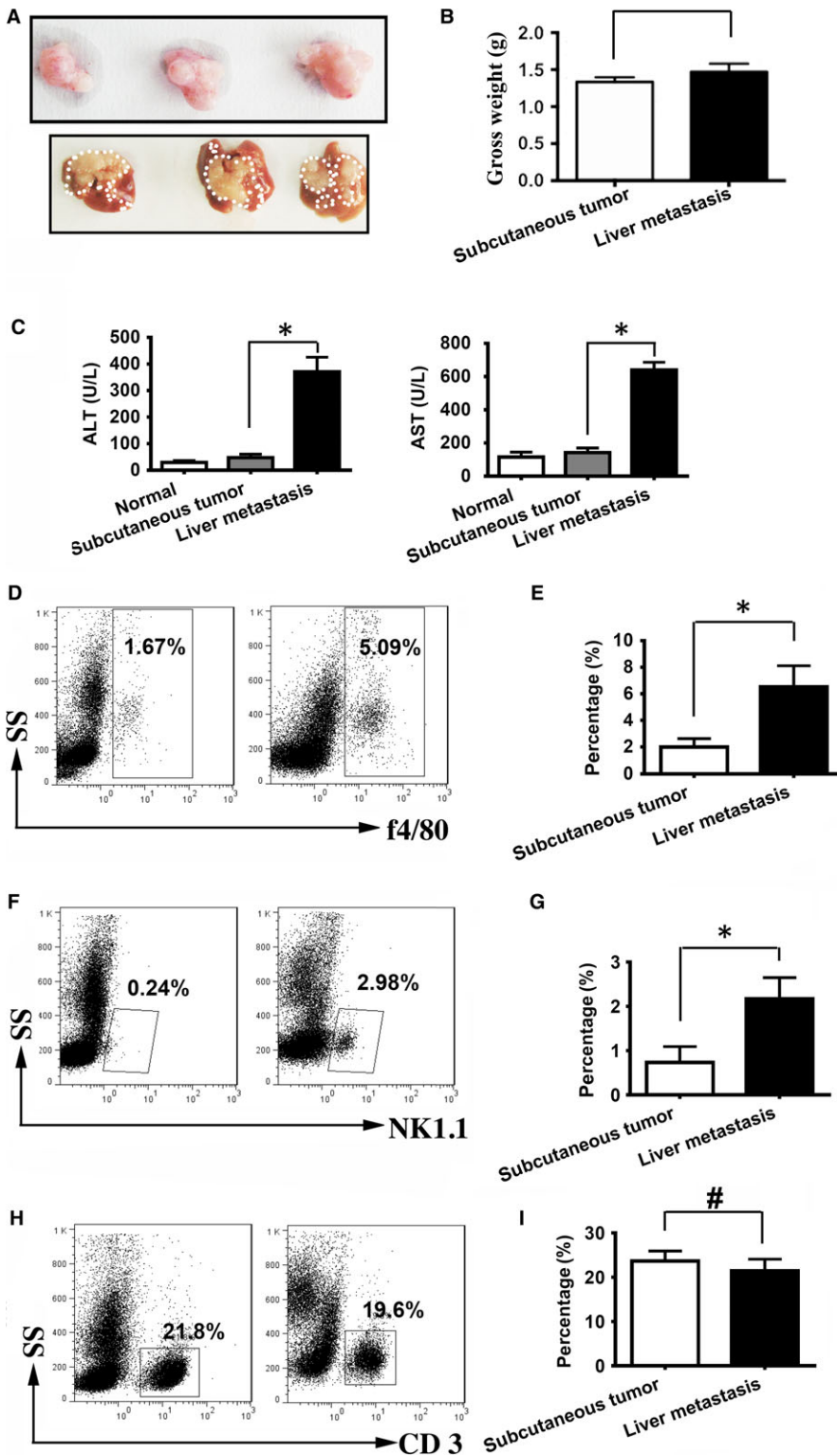


FIGURE 1 Compared to subcutaneous tumour, liver metastasis has more macrophage recruitment in blood corresponding to the liver injury. (A) Mouse colon cancer cells (SL4) were subcutaneously (top, 1×10^6) or splenic (below, 5×10^5) injected in C57 BL/6 WT mice. Subcutaneous tumour or tumour-bearing livers were harvested at 14 days after injection, respectively. (B) WT subcutaneous tumour or tumour-bearing livers were weighted, whose gross weight was similar. (C) The liver damage marker in blood, ie, ALT and AST was analysed. Liver metastasis caused much more serious liver injury. (D, E) Cytometry flow showed there was more F4/80⁺ macrophage recruitment in the blood of liver metastasis. (F, G) Cytometry flow showed there was more NK 1.1⁺ cells recruitment in the blood of liver metastasis. (H, I) Cytometry flow showed there was no difference of the CD3⁺ T cells in the blood of subcutaneous tumour and liver. $n = 6$, * $P < 0.05$; #No significant difference

results were obtained under the conditions that different numbers of SL4 cells were injected into the spleen of WT or AMPK α 2^{-/-} mice, resulting similar gross weight of tumour-bearing liver to avoid the interference of tumour size, because larger tumour size also leads to more liver damage.¹⁷ In this study, we injected the same number of SL4 cells into the spleen of WT or AMPK α 2^{-/-} mice to investigate the

roles of AMPK α 2 in liver damage and tumour-associated inflammation. First, our results showed that the deficiency of AMPK α 2 increased the tumour size, which was confirmed by the bioluminescence imaging (Figure 2A, B) and the gross weight of tumour-bearing liver (Figure 2C, D). The increased blood ALT and AST levels also indicated that AMPK α 2^{-/-} mice had more severe liver damage (Figure 2E, F).

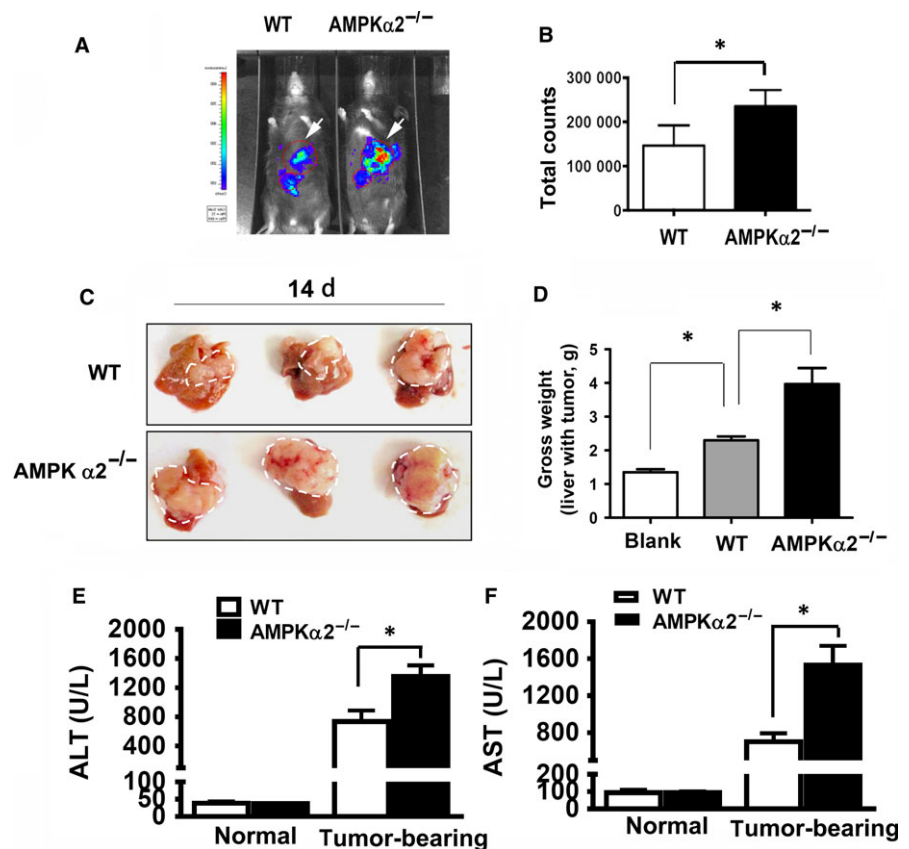


FIGURE 2 AMPK α 2 deficiency enhances tumour development of colon cancer cells in liver, which was positively associated with the more serious liver injury. (A) Bioluminescence imaging after D-luciferin injection on 12 days after SL4 injection showed the tumour location and size. (B) The analysis of total counts of bioluminescence imaging from the (A, arrowed area), $n = 3$. (C) Tumour-bearing liver of 14 days after intrasplenic injection of SL4 cells (5×10^5). (D) The analysis of the gross weight of tumour-bearing liver from (C), $n = 3$ -5. (E) The analysis of serum ALT and AST in WT and AMPK α 2^{-/-} mice corresponding to (A) ($n = 5$ -6). * $P < 0.05$; #No significant difference

3.3 | AMPK α 2 deficiency increases the number of macrophages in blood

To investigate the association between the enhanced liver injury and tumour-induced inflammation in the AMPK α 2 deficient mice, we analysed the proportions of CD3, CD3⁺/CD4⁺, CD3⁺/CD8⁺, F4/80⁺, NK1.1⁺ cells in the blood. As shown in Figure 3A, B, NK1.1⁺ cells did not show a significant difference in the blood of WT and AMPK α 2 deficient mice. However, total CD3 cells in blood decreased (Figure 3C, D), which was because of the reduction of CD3⁺/CD4⁺ cells (Figure 3G, H) but not CD3⁺/CD8⁺ cells (Figure 3E, F). And the CD3⁻/CD19⁺ cells showed no significant difference (data not shown). The decrease of blood CD4⁺ cells indicated more destruction of the immune system.³⁶ Notably, there was more blood microphage in the of AMPK α 2 deficient tumour-bearing mice, which was accompanied with a more serious liver injury. Thus, our results suggest that AMPK α 2 deficiency exacerbated tumour-related inflammation.

3.4 | AMPK α 2 deficiency exacerbates infiltration of inflammatory cells in the tumour

Then we analysed the immune cell infiltration, especially TAM in WT or AMPK α 2^{-/-} liver-bearing tumours. Our results of Mac-2 immunostaining showed that there are more tumour masses scatter in livers of AMPK α 2^{-/-} mice (Figure 4A). And much more Mac-2 positive Kuffer cells infiltrated into tumour tissues of AMPK α 2^{-/-} mice at day 10 (Figure 4A-C) and day 14 (Figure 4D). We also

checked the CD45⁺, F4/80⁺, CD4⁺, CD19⁺ cell populations in the tumours of WT or AMPK α 2^{-/-} mice at day 14 after colon cancer cell injection. Flow cytometry result showed that CD45⁺ cell populations increased significantly in the tumours of AMPK α 2^{-/-} mice (Figure 4E, F). Meanwhile, F4/80⁺ macrophages but not CD4⁺ cells increased significantly (Figure 4G-J).

3.5 | AMPK α 2 deficiency exacerbates the differentiation of M2 macrophages

Our previous results showed that AMPK α 2 deficiency enhanced the glucose deprivation in liver.¹⁷ AMPK is the sensor of energy deprivation.³⁷ It was unexpected to observe that the total AMPK α phosphorylation level was higher in AMPK α 2^{-/-} liver than in that of WT liver (Figure 5A), even though there was only AMPK α 1 and the total AMPK α was decreased in the liver of AMPK α 2^{-/-} mice (Figure 5B). And the expression of AMPK α 1 did not show a difference between control and AMPK α 2^{-/-} liver tissues (Figure 5B). It is well-established that AMPK α 1 but not AMPK α 2 is highly expressed in macrophages, and the enhanced activation of AMPK α 1 in macrophages increases the differentiation into the anti-inflammatory M2 type,^{26,28} which will promote the tumour progression.³⁸ It was obvious that there were many resident Kupffer macrophage cells in the a liver and the macrophages from blood were recruited into tumour areas (Figure 4C). Thus, we used mass spectrometry imaging to check the glucose deprivation in both liver and tumour of WT and AMPK α 2^{-/-} mouse. Our results showed that AMPK α 2^{-/-} liver had a more serious deprivation of

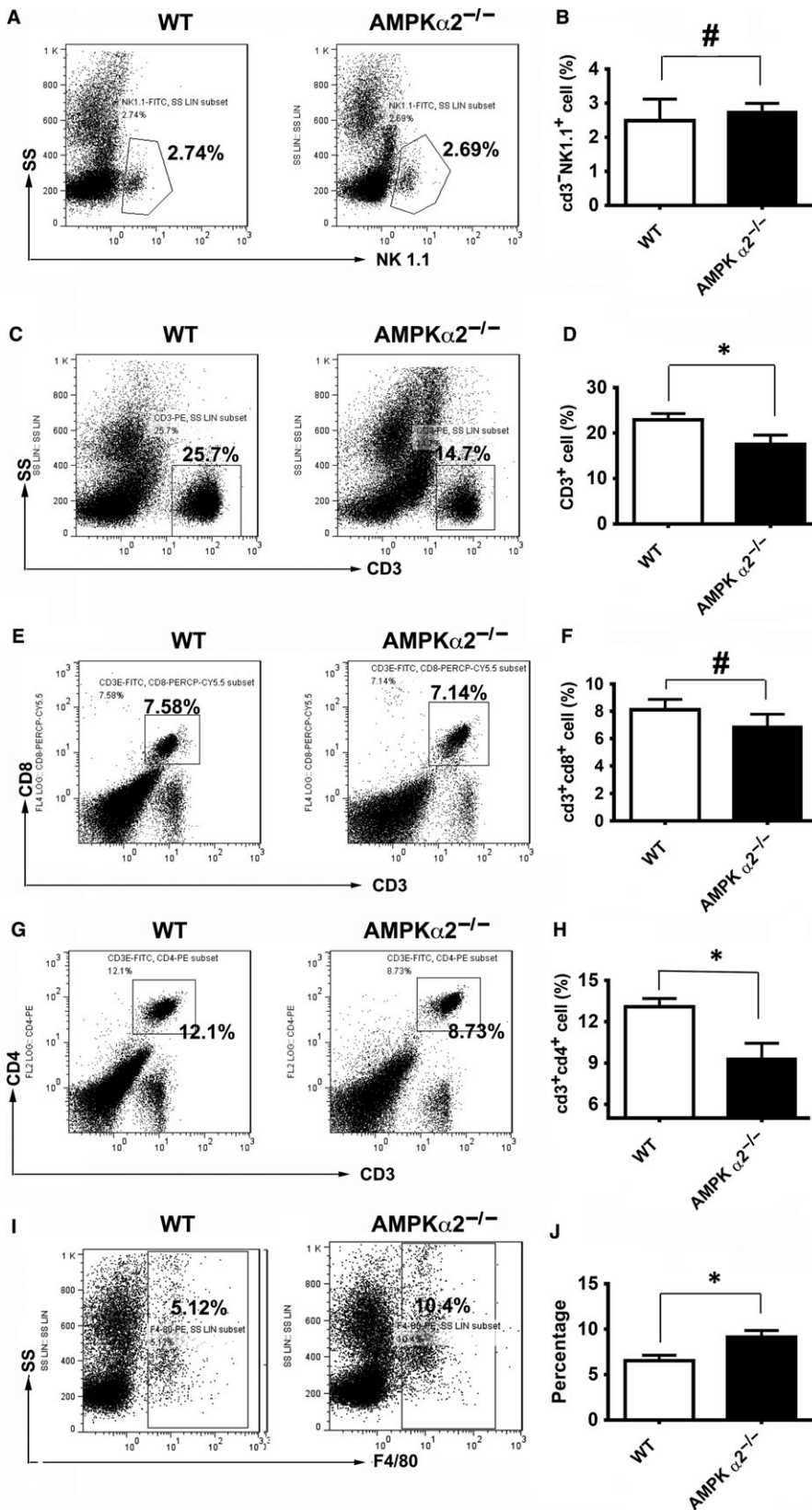


FIGURE 3 AMPK α 2 deficiency exacerbates the recruitment of macrophages in blood. (A, C, E, G, I) Representative flow-cytometry plots of NK1.1⁺ (A), CD3⁺ (C), CD3⁺CD8⁺(E), CD3⁺CD4⁺(G) T cells and F4/80⁺ (I) macrophages in blood of WT and AMPK α 2^{-/-} mice at day14 after colon cancer injection; (B, D, F, H, J) Quantification of NK1.1⁺ (B), CD3⁺ (D), CD3⁺CD8⁺(F), CD3⁺CD4⁺(H) T cells and F4/80⁺ macrophages (J) in WT and AMPK α 2^{-/-} mice blood. n = 3-6, *P < 0.05; #No significant difference

glucose than WT liver (Figure 5C, D). Another important result was that the glucose level in the small scattering tumour masses was similar to the surrounding liver tissue, but decreased drastically in the big tumour masses. Furthermore, both the glucose level of liver and

tumours in AMPK α 2^{-/-} mice were lower than those of WT mice, which is associated with the higher AMPK α phosphorylation level in the AMPK α 2^{-/-} liver. We then confirmed that the big tumour masses of AMPK α 2^{-/-} mice had more M2 type macrophages as shown by

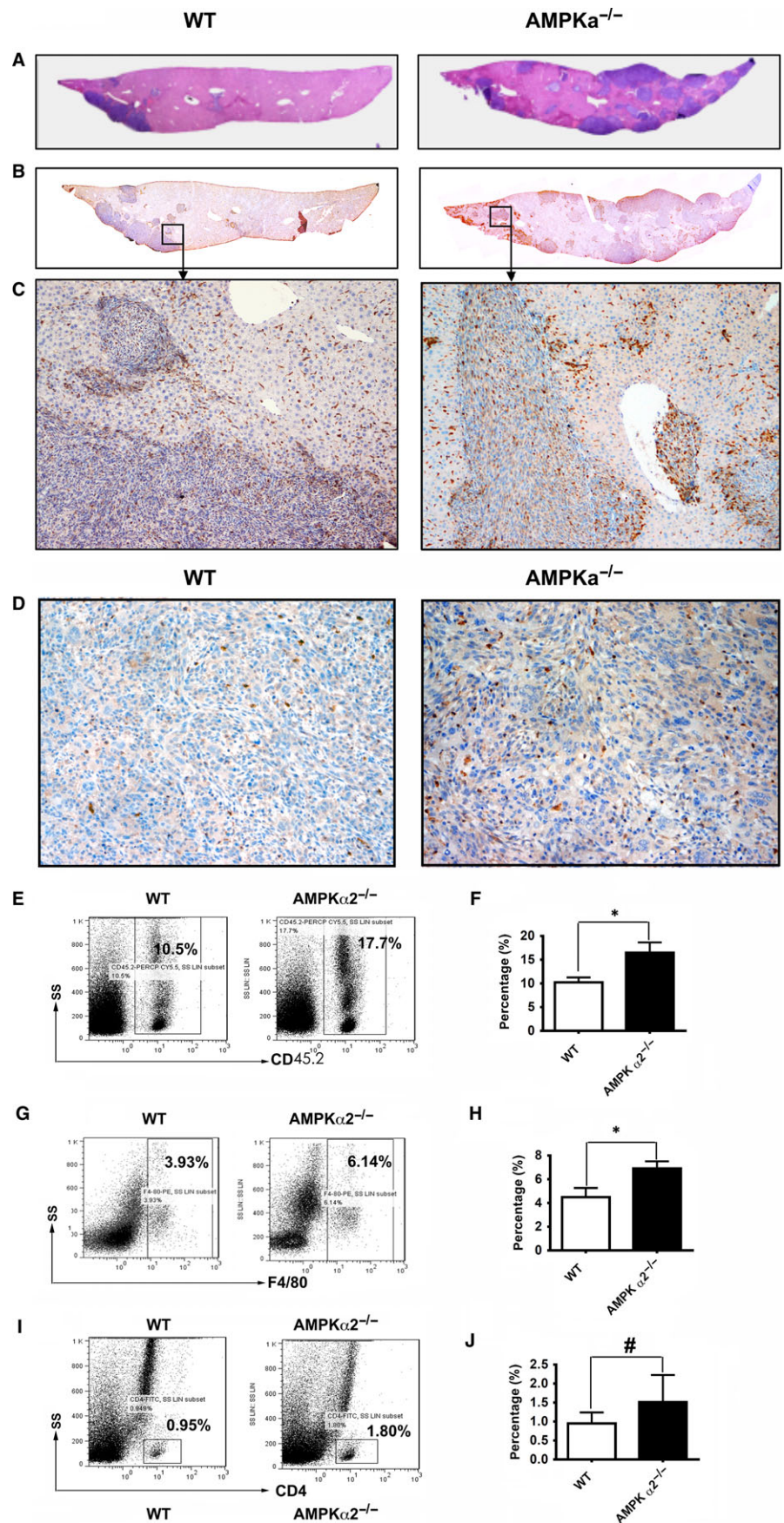


FIGURE 4 AMPK α 2 deficiency exacerbates infiltration of inflammation cells in tumour. (A, B, C) Haematoxylin and eosin (HE) (A) and IHC staining with Mac-2 antibody (B, C) at day 10; (D) IHC staining with Mac-2 antibody at day 14; (E, G, I) Representative result of flow-cytometry plots of CD45⁺(E), F4/80⁺ macrophages (G) and CD4⁺ T cell (I) in total cell suspensions from tumours of WT or AMPK α 2^{-/-} mice at day14 after colon cancer injection; (F, H, J) Quantification and statistical analysis corresponding to (E, G, I). n = 4-8. *P < 0.05, #no significant difference

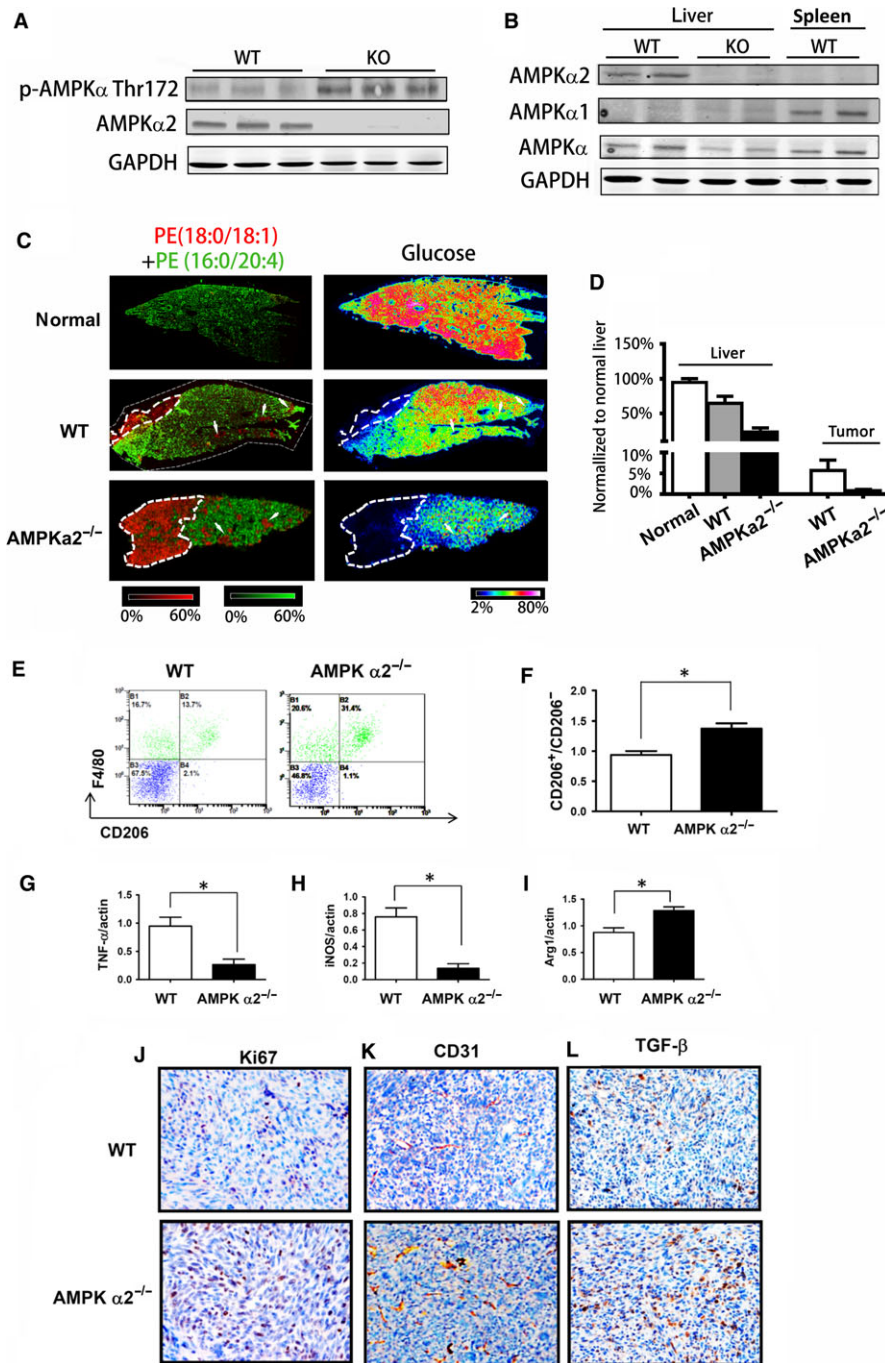


FIGURE 5 AMPK α 2 deficiency exacerbates M2 type macrophages differentiation. (A) Western blot analysis for p-AMPK α Thr172 and AMPK α 2 in liver of WT and AMPK α 2^{-/-} mice at day 14 after colon cancer injection; (B) Western blot analysis for AMPK α 2, AMPK α 1 and AMPK α expression in WT and AMPK α 2^{-/-} tumour-bearing liver, WT spleen as control; (C) Mass spectrometry imaging of glucose in normal liver and tumour-bearing liver of WT and AMPK α 2^{-/-} mice on day 14 after SL4 injection. Green is the false colour for glucose, Red is the false colour for tumour specific marker lipid as in³¹; (D) Quantification of the density of glucose in (C); (E, F) Flow-cytometry plots and quantification of the M2 marker protein CD206 in tumour cell suspension; (G, H, I) Expression of cytokine-related genes, TNF- α (G), INOS (H) and Arg1(I), analysed by quantitative RT-PCR; (J, K, L) IHC staining with Ki67(J), CD31(K) and TGF β (L) in WT and AMPK α 2^{-/-} tumour bearing liver. * $P < 0.05$

increased accumulation of CD206 positive macrophages (Figure 5E, F) and enhanced expression of M2 macrophages-associated cytokines (Figure 5G-I). Furthermore, the proliferation of tumour cells (Figure 5J), abnormal angiogenesis (Figure 5K) and TGF β expression (Figure 5L), were all increased in the big tumour of AMPK α 2^{-/-} mice, which corresponds to the anti-inflammatory tumour environment.

4 | DISCUSSION

The liver is the key organ controlling energy metabolism balance and acts as the most common organ for cancer metastasis. Many

cancers, especially colorectal cancer, can metastasize to liver tissues, and liver metastasis is the major cause of cancer mortality.^{33,39-41} Clinical investigations show that colorectal liver metastasis causes liver injury, especially at the advanced stage. Meanwhile, liver metastasis of colorectal cancer results in the increased inflammation which is related with patients' quality of life and mortality.^{42,43} Liver resection is one of the options after liver metastasis,^{44,45} but there are still many patients that can not be operated, and they suffer up until late-stage of liver metastasis. Although clinical studies report that liver metastasis is associated with liver injury,^{33,39,46,47} limited reports have indicated the mechanism. Our previous study showed that AMPK α 2 protects against liver injury from metastasized

tumours via reduced glucose deprivation-induced oxidative stress. Liver injury leads to inflammation, whereas inflammation further promotes liver injury.¹⁴ The inflammation acts as a propagator for tumour (reviews as^{15,48}). In this study, we focused on the molecular mechanism of liver injury and inflammation. We used a subcutaneous tumour model as a control of liver metastasis to study liver injury and inflammatory cell recruitment with or without liver metastasis. Our results showed that subcutaneous tumour xenograft without liver metastasis resulted in liver injury, but liver metastasis of colon cancer cells caused much more serious liver injury, which was associated with more recruitment of F4/80⁺ macrophages but not CD3⁺ T cells. This suggests that liver metastasis exacerbates inflammatory cells recruitment and liver injury.

AMPK is a heterotrimeric serine-threonine protein kinase, and it is conserved from yeast to mammals. The α subunit of AMPK is the catalytic subunit, which has at least two isoforms ($\alpha 1$ and $\alpha 2$) and can be phosphorylated by several upstream kinases, such as liver kinase B1 (LKB1), cAMP-dependent kinase (PKA), and Ca²⁺/CaM-dependent protein kinase II. AMPK is activated by multiple stress factors, including the energy stress and inflammatory environment. There are abundant reports showing that AMPK plays multiple roles in different tissues and disease conditions. The liver is enriched in AMPK $\alpha 2$ but not $\alpha 1$. Our previous report showed that liver injury was aggravated as the metastasized tumour expanded in the liver, and AMPK $\alpha 2$ deficiency enhanced the liver injury when the tumour sizes are similar in WT and AMPK $\alpha 2^{-/-}$ mice (injecting fewer cancer cells into AMPK $\alpha 2^{-/-}$ mice).¹⁷ Our present results showed that knockout of AMPK $\alpha 2$ enhanced the tumour growth and liver injury in the colon cancer cell liver metastasis mouse model (Figure 2). This suggests that the enhanced liver injury (injecting cancer cells of the same amount) in the AMPK $\alpha 2$ deficient mice is caused from both the bigger tumour size and the energy deprivation-related hepatocyte death. Correspondingly, AMPK $\alpha 2$ deficiency exacerbated macrophage but not NK1.1⁺ nature killer T cell recruitment in the blood (Figure 3), which suggests the more serious liver injury. We also observed that the CD3⁺CD4⁺ T cells but not CD3⁺CD8⁺ T cells were decreased in the blood of the AMPK $\alpha 2^{-/-}$ tumour-bearing mice (Figure 3). It has been reported that cancer patients with CD4 lymphopenia have an increased risk of severe toxicity after administration of cytotoxic chemotherapy and CD4 lymphopenia can indicate the worse immune condition and identify the end-of-life metastatic in cancer patients.³⁶ Thus, AMPK $\alpha 2$ deficient mice may exhibit the worse immune conditions, compared to the control mice.

Inflammation has recently been considered a hallmark of cancer and plays an important role in tumour initiation and progression.^{15,25,49} Tumour will recruit leucocytes and the polarization is one of the prominent events after leucocyte infiltration. In the tumour microenvironment, macrophages are one of the most abundant innate immune cells.^{18,21} Meanwhile, there are substantial clinical and experimental evidence showing that these macrophages generally exhibit similarities with polarized M2 macrophages, contributing to tumour growth, invasion, and angiogenesis.^{21,22} TAMs have served as a paradigm for cancer-related inflammation.^{22,38} The link between TAMs and tumour

development is well-established. Hence, we then analysed the infiltration of immune cells, including macrophages in the metastasized tumour in liver tissues. The F4/80⁺ macrophages were increased in the AMPK $\alpha 2^{-/-}$ mice at day 14 post tumour implantations. And CD19⁺ B cells were also increased. Correspondingly, the total immune cells, ie, CD45⁺ cells, were increased. Thus, comparing the results of immune cell recruitment and infiltration from blood and tumours, the increased immune cells in the tumour was not only because of the change of blood cell but also the tumour microenvironment of liver tissues affected by AMPK $\alpha 2$ deficiency.

AMPK has two catalytic isoforms AMPK $\alpha 1$ and $\alpha 2$, but they are tissue- and cell-specific expressed. Numerous studies have shown the total effect of AMPK $\alpha 1$ or $\alpha 2$ deletion on types of mouse models, however, there is a limited study to show whether AMPK $\alpha 1$ and $\alpha 2$ play different roles in the same disease conditions although they seem to be activated by the same stimuli.⁵⁰ Our previous results showed that AMPK $\alpha 2$ deficiency exacerbates the energy deprivation in AMPK $\alpha 2^{-/-}$ tumour-bearing liver.¹⁷ And we also reported that the glucose starvation in tumours is related with the tumour size and location. The glucose level was decreased significantly in the big tumour mass but not in the small tumour foci. And a glucose gradient was observed in large tumour, which implied a glucose competition between the tumour and liver remnant.³¹ Furthermore, AMPK is activated by energy stress.³⁷ It was not surprising that we observed the AMPK activation was higher in the tumour-bearing liver of AMPK $\alpha 2^{-/-}$ mice, although the deletion of AMPK $\alpha 2$ resulted in decreased total AMPK α and no significant AMPK $\alpha 1$ compensation (Figure 5B). Thus, it suggests that AMPK $\alpha 1$ was more strongly activated in AMPK $\alpha 2$ deleted tumour-bearing liver. It has been well-established that AMPK $\alpha 1$ activation in macrophages plays an anti-inflammatory effect.^{26,28} Correspondingly, we used glucose MS-imaging to reconfirm that the glucose level was more exacerbated in both tumour-bearing liver and tumour tissues of AMPK $\alpha 2^{-/-}$ mice than those of WT (Figure 5C). It is known that the infiltrated macrophages are not only from blood but also the resident macrophages, ie, Kuffer cells (Figure 4B, C). Then we confirmed that more infiltrated macrophage was polarized into M2 type macrophages, F4/80⁺/CD206⁺ macrophages (Figure 5G, H, I).

In summary, our study showed that the two isoforms of AMPK α , AMPK $\alpha 1$, and AMPK $\alpha 2$ in different cells exploit different ways to control tumour development in the liver. Although AMPK $\alpha 2$ plays anti-tumour effects, AMPK $\alpha 1$ in the macrophages may be activated in the tumour microenvironment and plays a pro-tumour effect. The total AMPK $\alpha 1$ knockout mice or condition knockout of AMPK $\alpha 1$ in immune cells will help further to exploit the AMPK $\alpha 1$ function in tumour environment in the future studies.

ACKNOWLEDGEMENTS

This study was supported by the National Natural Science Foundation of China (Grant Nos. 81570662, 81570215, 81400194, 81770468) and Wu Jieping Medical Foundation (Grand Nos. 320675017016).

CONFLICT OF INTEREST

The authors confirm that there are no conflicts of interests.

ORCID

Feng Lan  <http://orcid.org/0000-0002-9038-4014>

REFERENCES

- Hardie DG. Signal transduction: how cells sense energy. *Nature*. 2011;472:176-177. <https://doi.org/10.1038/472176a>.
- Hawley SA, Boudeau J, Reid JL, et al. Complexes between the LKB1 tumor suppressor, STRAD alpha/beta and MO25 alpha/beta are upstream kinases in the AMP-activated protein kinase cascade. *J Biol Chem*. 2003;281:4924-4924.
- Momcilovic M, Hong SP, Carlson M. Mammalian TAK1 activates Snf1 protein kinase in yeast and phosphorylates AMP-activated protein kinase in vitro. *J Biol Chem*. 2006;281:25336-25343.
- Woods A, Dickerson K, Heath R, et al. Ca²⁺/calmodulin-dependent protein kinase kinase-beta acts upstream of AMP-activated protein kinase in mammalian cells. *Cell Metab*. 2005;2:21-33.
- Zmijewski JW, Banerjee S, Bae H, Friggeri A, Lazarowski ER, Abraham E. Exposure to hydrogen peroxide induces oxidation and activation of AMP-activated protein kinase. *J Biol Chem*. 2010;285:33154-33164.
- Choi SL, Kim SJ, Lee KT, et al. The regulation of AMP-activated protein kinase by H₂O₂. *Biochem Biophys Res Comm*. 2001;287:92-97.
- Stapleton D, Mitchelhill KI, Gao G, et al. Mammalian AMP-activated protein kinase subfamily. *J Biol Chem*. 1996;271:611-614.
- Lihn AS, Jessen N, Pedersen SB, Lund S, Richelsen B. AICAR stimulates adiponectin and inhibits cytokines in adipose tissue. *Biochem Biophys Res Comm*. 2004;316:853-858.
- Cheung PC, Salt IP, Davies SP, Hardie DG, Carling D. Characterization of AMP-activated protein kinase gamma-subunit isoforms and their role in AMP binding. *Biochem J*. 2000;365:659-669.
- Viollet B, Foretz M, Guigas B, et al. Activation of AMP-activated protein kinase in the liver: a new strategy for the management of metabolic hepatic disorders. *J Physiol*. 2006;574:41-53.
- Jager S, Handschin C, St-Pierre J, Spiegelman BM. AMP-activated protein kinase (AMPK) action in skeletal muscle via direct phosphorylation of PGC-1alpha. *Proc Natl Acad Sci USA*. 2007;104:12017-12022.
- Hallows KR, Kobinger GP, Wilson JM, Witters LA, Foskett JK. Physiological modulation of CFTR activity by AMP-activated protein kinase in polarized T84 cells. *Am J Physiol Cell Physiol*. 2003;284:C1297-C1308.
- Evans AM, Mustard KJ, Wyatt CN, et al. Does AMP-activated protein kinase couple inhibition of mitochondrial oxidative phosphorylation by hypoxia to calcium signaling in O₂-sensing cells? *J Biol Chem*. 2005;280:41504-41511.
- Lohse AW, Weiler-Normann C, Tiegs G. Immune-mediated liver injury. *J Hepatol*. 2010;52:136-144.
- Grivennikov SI, Greten FR, Karin M. Immunity, inflammation, and cancer. *Cell*. 2010;140:883-899.
- Antonioni L, Blandizzi C, Pacher P, Hasko G. Immunity, inflammation and cancer: a leading role for adenosine. *Nat Rev Cancer*. 2013;13:842-857.
- Qiu SL, Xiao ZC, Piao CM, et al. AMP-activated protein kinase alpha2 protects against liver injury from metastasized tumors via reduced glucose deprivation-induced oxidative stress. *J Biol Chem*. 2014;289:9449-9459.
- Mantovani A, Sica A. Macrophages, innate immunity and cancer: balance, tolerance, and diversity. *Curr Opin Immunol*. 2010;22:231-237.
- Biswas SK, Sica A, Lewis CE. Plasticity of macrophage function during tumor progression: regulation by distinct molecular mechanisms. *J Immunol*. 2008;180:2011-2017.
- Oghumu S, Varikuti S, Terrazas C, et al. CXCR3 deficiency enhances tumor progression by promoting macrophage M2 polarization in a murine breast cancer model. *Immunology*. 2014;143:109-119.
- Murray PJ, Wynn TA. Protective and pathogenic functions of macrophage subsets. *Nat Rev Immunol*. 2011;11:723-737.
- Steidl C, Lee T, Shah SP, et al. Tumor-associated macrophages and survival in classic Hodgkin's lymphoma. *N Engl J Med*. 2010;362:875-885.
- Ahn GO, Tseng D, Liao CH, Dorie MJ, Czechowicz A, Brown JM. Inhibition of Mac-1 (CD11b/CD18) enhances tumor response to radiation by reducing myeloid cell recruitment. *Proc Natl Acad Sci USA*. 2010;107:8363-8368.
- Imtiyaz HZ, Williams EP, Hickey MM, et al. Hypoxia-inducible factor 2alpha regulates macrophage function in mouse models of acute and tumor inflammation. *J Clin Invest*. 2010;120:2699-2714.
- Sansone P, Bromberg J. Environment, inflammation, and cancer. *Curr Opin Genet Dev*. 2011;21:80-85.
- Yang Z, Kahn BB, Shi H, Xue BZ. Macrophage alpha1 AMP-activated protein kinase (alpha1AMPK) antagonizes fatty acid-induced inflammation through SIRT1. *J Biol Chem*. 2010;285:19051-19059.
- Brock SE, Rendon BE, Yaddanapudi K, Mitchell RA. Negative regulation of AMP-activated protein kinase (AMPK) activity by macrophage migration inhibitory factor (MIF) family members in non-small cell lung carcinomas. *J Biol Chem*. 2012;287:37917-37925.
- Sag D, Carling D, Stout RD, Suttles J. Adenosine 5'-monophosphate-activated protein kinase promotes macrophage polarization to an anti-inflammatory functional phenotype. *J Immunol*. 2008;181:8633-8641.
- Rao E, Zhang Y, Zhu G, et al. Deficiency of AMPK in CD8⁺ T cells suppresses their anti-tumor function by inducing protein phosphatase-mediated cell death. *Oncotarget*. 2015;6:7944-7958.
- Geissmann F, Manz MG, Jung S, Sieweke MH, Merad M, Ley K. Development of monocytes, macrophages, and dendritic cells. *Science*. 2010;327:656-661.
- Wang J, Qiu S, Chen S, et al. MALDI-TOF MS imaging of metabolites with a N-(1-naphthyl) ethylenediamine dihydrochloride matrix and its application to colorectal cancer liver metastasis. *Anal Chem*. 2015;87:422-430.
- Yang M, Liu J, Piao C, Shao J, Du J. ICAM-1 suppresses tumor metastasis by inhibiting macrophage M2 polarization through blockade of efferocytosis. *Cell Death Dis*. 2015;11:144.
- Seve P, Ray-Coquard I, Trillet-Lenoir V, et al. Low serum albumin levels and liver metastasis are powerful prognostic markers for survival in patients with carcinomas of unknown primary site. *Cancer*. 2006;107:2698-2705.
- Malhi H, Gores GJ. Cellular and molecular mechanisms of liver injury. *Gastroenterology*. 2008;134:1641-1654.
- Liaskou E, Wilson DV, Oo YH. Innate immune cells in liver inflammation. *Mediators Inflamm*. 2012;2012:949157.
- Peron J, Cropet C, Tredan O, et al. CD4 lymphopenia to identify end-of-life metastatic cancer patients. *Eur J Cancer*. 2013;49:1080-1089.
- Hardie DG. AMP-activated/SNF1 protein kinases: conserved guardians of cellular energy. *Nat Rev Mol Cell Biol*. 2007;8:774-785.
- Dehne N, Mora J, Namgaladze D, Weigert A, Brune B. Cancer cell and macrophage cross-talk in the tumor microenvironment. *Curr Opin Pharmacol*. 2017;35:12-19.
- Ochiai H, Nakanishi Y, Fukasawa Y, et al. A new formula for predicting liver metastasis in patients with colorectal cancer: immunohistochemical analysis of a large series of 439 surgically resected cases. *Oncology*. 2008;75:32-41.
- Trivanovic D, Petkovic M, Stimac D. New prognostic index to predict survival in patients with cancer of unknown primary

- site with unfavourable prognosis. *Clin Oncol (R Coll Radiol)*. 2009;21:43-48.
41. Lazaridis G, Pentheroudakis G, Fountzilas G, Pavlidis N. Liver metastases from cancer of unknown primary (CUPL): a retrospective analysis of presentation, management and prognosis in 49 patients and systematic review of the literature. *Cancer Treat Rev*. 2008;34:693-700.
 42. Huang A, Fuchs D, Widner B, Glover C, Henderson DC, Allen-Mersh TG. Serum tryptophan decrease correlates with immune activation and impaired quality of life in colorectal cancer. *Br J Cancer*. 2002;86:1691-1696.
 43. Earlam S, Glover C, Fordy C, Burke D, Allen-Mersh TG. Relation between tumor size, quality of life, and survival in patients with colorectal liver metastases. *J Clin Oncol*. 1996;14:171-175.
 44. Fan J, Wu ZQ, Tang ZY, et al. Complete resection of the caudate lobe of the liver with tumor: technique and experience. *Hepatogastroenterology*. 2001;48:808-811.
 45. Heinrich S, Lang H. Liver metastases from colorectal cancer: technique of liver resection. *J Surg Oncol*. 2013;107:579-584.
 46. Mielczarek M, Chrzanowska A, Scibior D, et al. Arginase as a useful factor for the diagnosis of colorectal cancer liver metastases. *Int J Biol Markers*. 2006;21:40-44.
 47. Yeo SG, Kim DY, Kim TH, Kim SY, Hong YS, Jung KH. Whole-liver radiotherapy for end-stage colorectal cancer patients with massive liver metastases and advanced hepatic dysfunction. *Radiat Oncol*. 2010;5:97.
 48. Hanahan D, Weinberg RA. Hallmarks of cancer: the next generation. *Cell*. 2011;144:646-674.
 49. Albini A, Sporn MB. The tumour microenvironment as a target for chemoprevention. *Nat Rev Cancer*. 2007;7:139-147.
 50. Violette B, Athes Y, Mounier R, et al. AMPK: lessons from transgenic and knockout animals. *Front Biosci (Landmark Ed)*. 2009;14:19-44.

How to cite this article: Qiu S, Liu T, Piao C, et al. AMPK α 2 knockout enhances tumour inflammation through exacerbated liver injury and energy deprivation-associated AMPK α 1 activation. *J Cell Mol Med*. 2019;23:1687–1697.
<https://doi.org/10.1111/jcmm.13978>